Phys. Status Solidi A **212,** No. 8, 1767–1773 (2015) / **DOI** 10.1002/pssa.201431845

physica status solidi a
www.pss-a.com
applications and materials science

Influence of the presence of Ca in the cathode buffer layer on the performance and stability of organic photovoltaic cells using a branched sexithienylenevinylene oligomer as electron donor

Francisco Martinez[1], Gloria Neculqueo[1], Jean Christian Bernède[*,2], Linda Cattin[3], and Mohammed Makha[2]

[1] Departamento de Ciencia de los Materiales, Facultad de Ciencias Físicas y Matemáticas, Universidad de Chile, Casilla 2777, Santiago, Chile
[2] Université de Nantes MOLTECH-Anjou, CNRS, UMR 6200, 2 rue de la Houssinière, BP 92208, 44000 Nantes, France
[3] Institut des Matériaux Jean Rouxel (IMN), Université de Nantes, CNRS, UMR 6502, 2 rue de la Houssinière, BP 32229, 44322 Nantes cedex 3, France

Received 18 November 2014, revised 23 February 2015, accepted 23 February 2015
Published online 18 March 2015

Keywords branched sexithienylenevinylene oligomer, buffer layers, heterojunctions, lifetime, organic solar cells

[*] Corresponding author: e-mail jean-christian.bernede@univ-nantes.fr, Phone/Fax: +33 251 125 530

A new branched sexithienylene vinylene oligomer, (E)-bis-1,2-(5,5″-dimethyl-(2,2′:3′,2″-terthiophene)vinylene (BSTV), was synthesized, characterized, and used as the electron donor in a planar heterojunction organic photovoltaic cell (OPVC). The OPVC utilized fullerene (C_{60}) as the electron acceptor, ITO-coated glass as the anode, and aluminum as the cathode. Hybrid electrode buffer layers of MoO_3/CuI on the anode side and of Alq_3/Ca on the cathode side were used. This shows the effectiveness of the bilayer Alq_3/Ca as a cathode buffer layer. The thickness of the Ca layer and its effect on the performance and lifetime of the OPVCs were studied. It was found that an Alq_3/Ca structure with 6 nm of Alq_3 and 3 nm of Ca has an efficiency (η) of 2.28%, while a device without Ca has an efficiency of only 1.47%. Combining an optimized thickness of the new donor BSTV (22 nm) together with the bilayer cathode buffer layer, a device having an open-circuit voltage, V_{oc} of 0.84 V, a short-circuit current, J_{sc} of 3.60 mA cm^{-2}, and a fill factor, FF of 50% was achieved. However, the efficiency of the OPV with Ca decreases rapidly during the first hours of air exposure, resulting in device performance that is similar to a device fabricated without Ca. After this initial degradation, device performance for both types of OPV evolves similarly with continued air exposure.

1 Introduction Organic photovoltaic cells (OPVCs) have received a great attention due to their potential as inexpensive sources of renewable energy. Different cell configurations are employed to improve photon absorption, charge separation, and transport in organic solar cells [1–3].

Small-molecule OPVCs are classically based on an organic bilayer sandwiched between two electrodes [4]. One of these electrodes must be transparent and the other must be highly reflective. The bilayer heterojunction consists of an electron-donor (ED) layer adjacent an electron-acceptor (EA) layer. Regarding the electrodes, while aluminum is often used as the reflective cathode, indium tin oxide (ITO) is often used as the transparent conductive anode. Small molecules offer several advantages over polymeric materials, such as more facile synthesis and purification, inherent monodispersity, and high tenability [5].

Carrier exchange at the organic material/electrode interfaces is often a limiting factor for device performance.

The yield of hole collection by the anode must be high, while it must be electron selective and the reverse must be true at the cathode side. Ideally, the donor's HOMO (highest occupied molecular orbital) should match the work function of the anode [6–11] and the LUMO (lowest unoccupied molecular orbital) should match the work function of the cathode.

Moreover, it is important to keep in mind that the efficiency is only one of the criteria for the commercialization of OPVCs. Another important one is their stability.

In the present work, we present a new ED as the absorbing layer and a new hybrid cathode buffer layer. The influence of this new buffer layer on the OPVCs lifetime is studied.

The new absorber of light is the branched sexithienylenevinylene oligomer (BSTV) (Fig. 1). It is known that oligothiophenes and derivatives are among the most promising organic semiconducting materials because of their good transport properties, as well as their tunable optical properties [12]. Moreover, in order to achieve low-cost devices, it is important to choose new molecules that exhibit high synthetic yield, which is the case for BSTV. All these advantages justify our choice.

A planar heterojunction OPVC is presented. Planar heterojunctions are well suited for investigating new materials, as materials can be characterized independently before device fabrication and many parameters, such as light absorption and film morphology, can be determined experimentally. So, after briefly recalling the chemical synthesis of the BSTV, the properties of the BSTV thin films deposited onto the transparent electrode are presented.

At the cathode/EA interface, a cathode buffer layer (CBL) was introduced. Usually, this CBL consists of a wide-bandgap organic layer. This layer has been called the exciton blocking layer (EBL) because its bandgap is substantially larger than those of the organic donor and acceptor. The EBL blocks excitons in the organic layer far from the cathode, avoiding any quenching effect at the cathode/organic interface [13]. More precisely, the enhancement of OPVCs performance in the presence of this EBL is attributed not only to the blocking of excitons but also to the prevention of metal–atom diffusion into the organic electron acceptor during the deposition of the cathode. If the EBL blocks excitons, it should not block all charge carriers. However, the offset energy of the highest occupied molecular orbital (HOMO) of the electron acceptor (often the fullerene) and the EBL (such as bathocuproine or aluminum tris(8-hydroxyquinoline (Alq_3)) is large. Moreover, the optimum EBL thickness is 9 ± 1 nm, which is too thick to allow high tunneling currents. So, it has been suggested that the charge transport in the EBL is due to aluminum diffusion during deposition of the cathode [13–15]. Al diffusion can introduce conducting levels in the EBL bandgap, which explains why the transport of electrons through the CBL is possible. However, it does not ensure optimum extraction of electrons, as is obtained by using a low work function cathode such as Ca [16–18]. Nevertheless, due to small exciton diffusion lengths, the active organic layers in planar heterojunctions must be thin, which means that it is necessary to use a reflective cathode in order to improve light absorption. Unfortunately, a thick Ca layer (20–40 nm) exhibits low reflectivity and so it cannot be used as the cathode. Therefore, in the present work we propose to use a hybrid CBL, EBL/Ca, in order to try to combine the benefits of both a EBL and a Ca electrode.

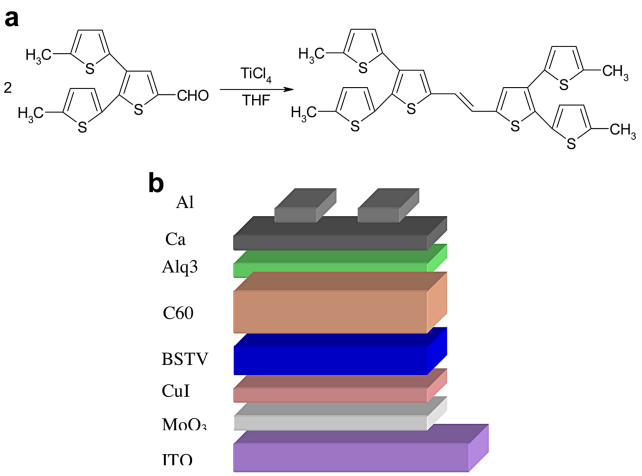

Figure 1 (a) Synthesis of BSTV, (b) sketch of the OPVC.

Actually, after optimization of the thickness of the branched sexithienylenevinylene absorbing layer (BSTV), we show that higher device efficiency is achieved with the EBL/Ca hybrid CBL compared to devices utilizing the EBL alone. However, the study of the lifetime of the OPVCs using simple EBL or hybrid EBL/Ca CBL shows that, with time, the presence of Ca to be efficient requires a highly efficient encapsulation.

2 Experimental

2.1 Synthesis of (E)-bis-1,2-(5,5″-dimethyl-(2,2′:3′,2″-terthiophene)vinylene (BSTV) The synthesis and characterization of BSTV has been previously described [19]. In fact, the (E)-bis-1,2-(5,5″-dimethyl-(2,2′:3′,2″-terthiophene)vinylene (BSTV) was synthesized from 5,5″-dimethyl-2,2′.3′,2″-terthiophene-5′-carbaldehyde following the procedure described in Ref. [20].

The product was purified by column chromatography on silica gel using hexane as the eluent, yielding a yellow-orange solid (0.81 g; 86% yield). FT-IR (KBr, cm^{-1}): 3065, 3004, 2912, 2854, 1749, 1616, 1535, 1476, 1436, 1374, 1192, 1156, 1031, 924, 837, 794, 617, 564, 520, 418. ^{1}H-NMR ($CDCl_3$, 300 MHz): δ (ppm) 7.02 (2H, s), 6.97 (2H, d, $J = 3.5$ Hz), 6.92 (2H, s), 6.89 (2H, d, $J = 3.5$ Hz), 6.67 (4H, m), 2.49 (12H, m). ^{13}C-NMR ($CDCl_3$, 75 MHz): δ (ppm) 141.5, 140.2, 139.8, 134.8, 132.8, 132.0, 130.9, 129.3, 127.6, 126.7, 125.5, 125.3, 121.3, 15.47, 15.43, HRMS (MALDI-TOF) calculated for $C_{30}H_{24}S_6^+$, 576.9071; found: 576.0210.

2.2 Solar-cell fabrication The ITO-coated glass substrates were obtained from SOLEMS. The standard substrate dimensions were 25 mm by 25 mm. As ITO covered the whole glass substrate, some ITO must be removed to obtain the under electrode. A 25 mm by 17 mm section of each substrate was masked; ITO was then etched using Zn + HCl [21].

After scrubbing with soap, the substrates were rinsed in running deionized water, dried under an argon flow, and then loaded into a vacuum chamber (10^{-4} Pa).

As described above, the electron donor was BSTV (Fig. 1). The fullerene C_{60} was used as the electron acceptor and the cathode was an aluminum film. The ABL was the double layer MoO_3/CuI. We have already shown that this double ABL allows optimized efficiencies to be achieved [10]. The EBL used in the CBL was the aluminum tris(8-hydroxyquinoline) (Alq_3). Alq_3 was chosen because it has been shown that it allows fabrication of solar cells with increased lifetimes. Moreover, it has been proven to be a very efficient EBL [22, 23]. The second layer of the hybrid CBL is a thin layer of Ca. The typical thickness of the CBL in planar heterojunction-based OPVCs is 9 ± 1 nm, so we choose 6 nm as the thickness of the Alq_3, while the Ca thickness was varied from 2 to 4 nm.

Chemicals were provided by either Aldrich or CODEX (France). They were used without any purification. Indeed, it has been shown that using the same charge in the evaporation crucible, there is an "autopurification" of the product during vacuum thin-film depositions [24].

MoO_3, CuI, BSTV, C_{60}, Alq_3, Ca, and Al were deposited under a vacuum of 10^{-4} Pa. The thin-film deposition rates and thickness were estimated *in situ* with a quartz monitor. The deposition rate and the thickness of the MoO_3 layer were 0.02 nm s^{-1} and 3 nm, respectively [9]. The deposition rate of CuI has a large influence on the properties of the cells [25]. Actually, it is necessary to deposit this film very slowly to prevent current leakage effects. Therefore, the CuI film was deposited at a rate of 0.005 nm s^{-1} and its thickness was limited at 1.5 nm. The deposition rate and thickness for C_{60} were 0.05 nm s^{-1} and 40 nm, respectively. The deposition rates of BSTV, Alq_3, and Ca were 0.05, 0.1, and 0.02 nm, respectively. The fixed thicknesses were chosen after preceding optimizations [21]. After organic thin-film deposition, the aluminum top electrodes were thermally evaporated, without breaking the vacuum, through a mask with 2–8 mm active areas. In the present work, the effect of the thickness of the BSTV film on the solar-cell performance was first studied using a simple EBL layer of Alq_3. The hybrid CBL was then probed.

Finally, the device structures used were: glass/ITO(100 nm)/MoO_3(3 nm)/CuI(1.5 nm)/BSTV (y nm)/C_{60}(40 nm)/CBL/Al(120 nm), with CBL = Alq_3 (6 nm)/Ca (x nm) (Fig. 1b).

2.3 Characterization techniques ^{1}H-NMR and ^{13}C-NMR spectra were recorded on a Bruker 300 MHz (^{1}H: 300 MHz; ^{13}C: 75 MHz) spectrometer using deuterated chloroform as solvent. High-resolution mass spectra were recorded on an ESI-TOF LCT Premier XE mass spectrometer.

Electrical characterizations were performed with an automated *I–V* tester, in the dark and under global sun AM 1.5 simulated solar illumination. Performances of photovoltaic cells were measured using a calibrated solar simulator (Oriel 300 W) at 100 mW cm^{-2} light intensity adjusted with a PV reference cell (0.5 cm^2 CIGS solar cell, calibrated at NREL, USA). Measurements were performed under an ambient atmosphere. All devices were illuminated through TCO electrodes.

The morphology and film cross sections were observed through scanning electron microscopy (SEM) with a JEOL 6400 F at the "Centre de microcaractérisation de l'Université de Nantes." Optical transmission spectra were recorded by a Cary spectrophotometer. The optical transmission was measured at wavelengths of 2–0.25 μm.

3 Experimental results The morphology of the thin film of BSTV is very homogeneous (Fig. 2), which allows leakage currents in OPVCs to be prevented. The absorption

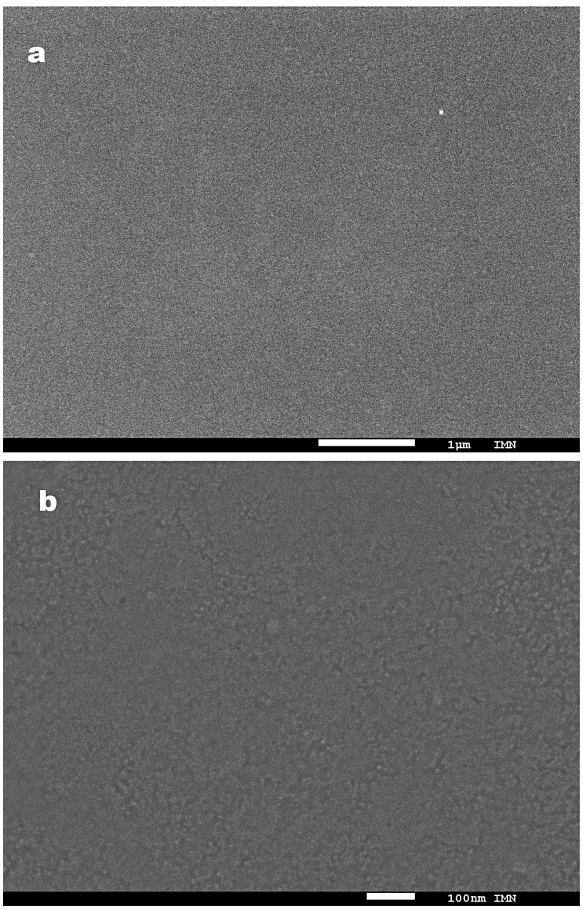

Figure 2 Microphotographs of a BSTV film (22 nm) deposited onto a glass/ITO/MoO_3/CuI structure, (a) low magnification, (b) high magnification.

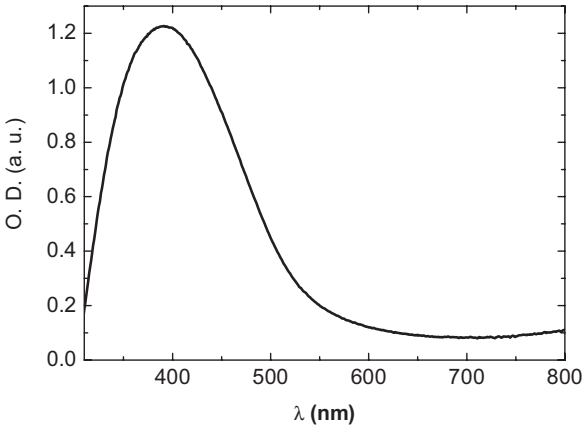

Figure 3 Optical absorption of BSTV in thin films.

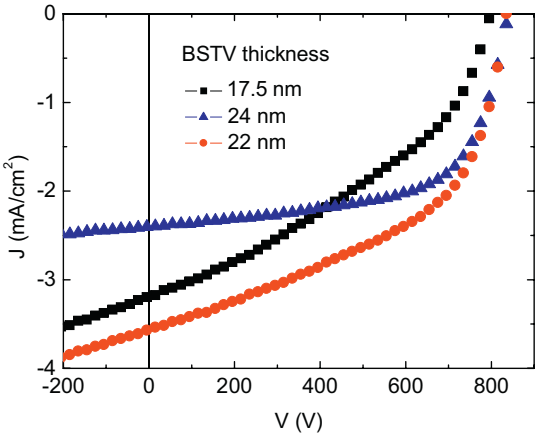

Figure 4 Typical *J–V* characteristics of OPV cells with BSTV film thickness of 17.5 nm (■), 22 nm (●), and 24 nm (▲).

spectrum of the thin film of BSTV is shown in Fig. 3. One can see that the threshold absorption value is around 538 nm. It can be estimated roughly that this threshold energy corresponds to the optical bandgap of the BSTV thin films, which means that its bandgap is about 2.30 eV.

After these characterizations, the BSTV was introduced, as an electron-donor layer, in OPVCs. First, a systematic study of the influence of the BSTV thickness (t) on the OPVCs performances was done by varying the thickness from $t = 17.5$ to 24 nm. Figure 4 shows the *I–V* characteristics of typical organic solar cells with BSTV thickness of 17.5, 24, and 22 nm. The open-circuit voltage (V_{oc}), the short-circuit current density (J_{sc}), the fill factor (FF), and the cell power conversion efficiency (η) are presented in Table 1. The results presented correspond to critical BSTV thicknesses. The optimum efficiencies are achieved for a BSTV film thickness of 22 nm. For a thinner ED film, all the OPV cell parameters decrease with a strong FF degradation. For thicker ED films, FF continues to increase, while J_{sc} decreases significantly, resulting in a decrease of the OPVC efficiency. Since we showed that the CuI ABL allows improving the current of the OPV cells [10, 25], we tried to circumvent the negative effects of increasing the thickness of BSTV on the series resistance (Table 1) by increasing the thickness of CuI. It can be seen from Table 1 that, as expected, the series resistance is significantly decreased, which results in a significant improvement in the short-circuit current. However, simultaneously, the shunt resistance is strongly decreased, which induces significant degradation of the open-circuit voltage and fill factor, and finally of the OPVC efficiency. Therefore, as already shown the more efficient DABL consists of the MoO_3/CuI structure with 1.5 nm of CuI, while the optimum BSTV thickness is 22 nm.

After this optimization we substitute for the simple Alq_3 EBL, the hybrid CBL Alq_3/Ca structure.

The influence of the Ca thickness on the *J–V* characteristics of the OPVCs under illumination is presented in Fig. 5. It can be seen that the optimal thicknesses correspond to 6 nm of Alq_3 and 3 nm of Ca, with $V_{oc} = 0.84$ V, $J_{sc} = 5.66$ mA/cm^2, FF = 48%, and $\eta = 2.28\%$. We attribute this performance improvement to the electron-blocking ability of Alq_3 and the improved band matching at the EA/cathode interface by using Ca.

Then, we proceeded to study the lifetime of the different optimized OPVCs. To improve the accuracy of the aging study, the OPVCs were "semiencapsulated." Actually, without adding a protecting layer the performance of OPVCs are known to decline rapidly [26]. In order to limit this instability, an encapsulating layer of amorphous selenium (Se-a) was thermally evaporated before exposing the devices to atmospheric conditions. Selenium protective coatings have been proven to efficiently protect the devices against oxygen and water [27] for at least a few hours in air, depending on thickness [28]. The longer lifetime of the devices thus obtained allows a more precise analysis of the effects causing degradation. Following the protocol

Table 1 Photovoltaic performance data under AM1.5 conditions of solar cells with different BSTV thicknesses.

BSTV thickness (nm)	CuI thickness (nm)	V_{oc} (V)	J_{sc} (mA/cm^2)	FF (%)	η (%)	R_s (Ω)	R_p (Ω)
17.5	1.5	0.80	3.13	38	0.97	26	560
22	1.5	0.84	3.60	50	1.47	24	660
24	1.5	0.84	2.40	63	1.27	45	2400
24	3.0	0.65	5.05	37	1.22	9	250

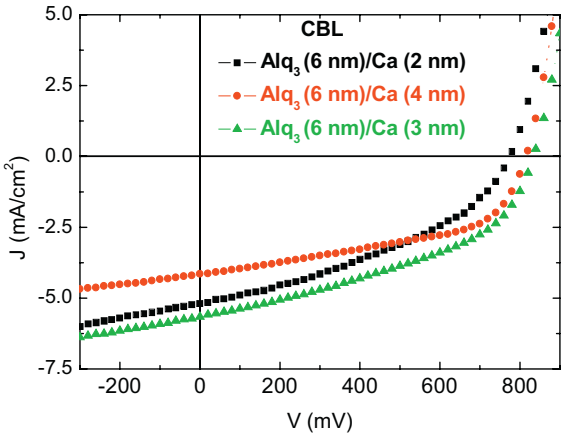

Figure 5 Typical J–V characteristics of OPV cells with different Ca thickness in the CBL Alq_3 (6 nm)/Ca (x nm): $x = 2$ nm (■), 3 nm (▲), and 4 nm (●).

proposed in Ref. [29], the procedure used to study the aging process of our OPVCs corresponds to the intermediate level labeled "Level 2." The operational lifetimes were measured under AM1.5, in air and at room temperature. Between each measurement, samples were stored in air and in the light of day, the cells being in open circuit conditions.

OPVC efficiency losses are typically due to decreases in V_{oc} and FF. In the present study, the most striking effect is the very fast decrease of the efficiency of the OPVCs with Ca in their CBL. Actually, as can be seen in Fig. 6, after this fast initial decrease, the efficiency of these OPVCs follows the same evolution as those without Ca. This indicates that the improvement due to the presence of Ca is quickly offset by air contamination. It was shown that, when they are kept in nitrogen, OPVCs using Ca as the buffer layer show a good stability and that a better stability is expected for encapsulated devices [17]. So, to prevent fast degradation and to maintain the device performance improvement due to Ca, it will be necessary to carefully encapsulate the OPVCs.

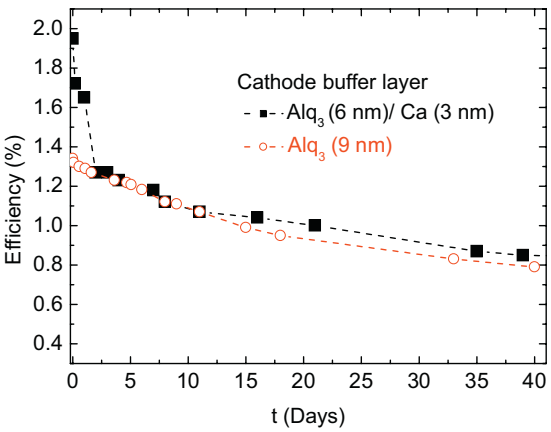

Figure 6 Variation with time of the efficiency of OPVCs with different CBL: with (■) and without Ca (○).

4 Discussion The J–V characteristics measured in the dark show that the OPV cells studied exhibit the typical rectifying shape of a diode with a high turn-on voltage value. This high turn-on voltage allows high V_{oc} to be obtained when the device is submitted to light irradiation.

The V_{oc} gradually increases as the BSTV thickness increases, which is in agreement with a previous study [30]. As a matter of fact, the organic film thickness being very small, any default in its growth may induce V_{oc} limitations. When the organic film thickness increases, there is a decrease in the impact of these side effects on V_{oc}.

The short-circuit current is limited by light absorption, the charge separation, and the collection efficiency. It is known that organic materials have very high absorption coefficients so that only 100-nm thick films are necessary to absorb the light if a reflective back contact (such as aluminum) is used. After photon absorption and exciton formation, the excitons must reach an ED/EA interface for dissociation. However, the exciton diffusion length in organic materials is approximately 10–15 nm, which means that the distance between an exciton–creation site and the interface should not be higher than this length. Moreover, after charge separation they must be collected by the electrodes, knowing that charge mobility is very low in organic materials. As a result, it is necessary to determine a thickness that allows the best compromise between the absorption of photons and the collection of charge carriers to be obtained.

The slopes at the short-circuit point and at the open-circuit voltage are the inverse values of the shunt resistance (R_{sh}) and the series resistance (R_s), respectively, of an equivalent circuit scheme of a solar cell (Table 1). With BSTV thickness increasing up to 22 nm, R_s and R_{sh} do not vary strongly and J_{sc} increases slowly with the increasing thickness. Beyond 22 nm, R_s and R_{sh} increase significantly and J_{sc} decreases strongly, indicating that the charge collection and optical absorption were maximized at a BSTV thickness of 22 nm. Surprisingly, the FF value increases continuously with the increasing BSTV thickness. A high FF can be attributed to low R_s or high R_{sh} [31]. We can see from Table 1 that R_{sh} increases fourfold while R_s is not even doubled, which may explain this evolution of FF.

With respect to the large change in J_{sc} for a 2-nm difference of ED BSTV (Table 1), it can also be seen from Table 1 that the modification of the CuI thickness strongly affects the parameters of the cells. A significantly higher J_{sc}, with smaller V_{oc} and FF is observed, when the CuI thickness changes from 1.5 to 3 nm. So, we cannot exclude that, perhaps, the layer of CuI, for the example given in Table 1, in the case of 22-nm BSTV, is slightly less than the 1.5 nm announced. For this thickness, there is some small error (±0.3 nm) of the quartz monitor. A smaller CuI thickness could contribute, in addition to that of the BSTV thickness, to the large change of the value of J_{sc} in Table 1.

As shown in Table 1, a thicker CuI film yields a device that has a large increase in J_{sc} while the V_{oc} and FF decrease,

resulting in a smaller OPV cell efficiency. The variation of the different parameters of these cells is in good agreement with the evolution of R_s and R_{sh}. Actually, the value of R_s is the smallest obtained in this work, which justifies the high J_{sc} value, while R_{sh} is the smallest ever obtained, which justifies the small value of FF and V_{oc}. As we have already shown that CuI improves the conductivity of the organic films [32], it also tends to grow nonuniformly [33], which can induce shunt paths across the device, which decreases R_s and R_{sh}. The present study confirms that the optimum CuI thickness is 1.5 nm when it is deposited at 0.005 nm s^{-1}.

The improvement due to Ca introduction in the CBL can be discussed on the basis of the dual functions of Alq_3 and Ca. While Alq_3 behaves as an EBL, Ca reduces the electron-injection barrier due to its small work function (2.9 eV).

As described above, in the case of classical OPVCs, it has been proposed that the EBL not only blocks the exciton, but it can also protect the electron-accepting film from atoms' diffusion during deposition of the electrode. During electrode deposition onto the organic material, Al diffusion can introduce conducting levels within the EBL bandgap and may explain why electron transport is not weakened despite the thickness of the EBL. The optimum thickness is justified by the fact that, if it must be thick enough to protect the electron-accepting layer from metal atom diffusion, it must also not block all charge carriers. Therefore, the EBL thickness should be chosen so that it allows electron collection at the cathode and prevents electron acceptor contamination by metal atoms.

The low work function of Ca is expected to improve the band matching at the electron acceptor/cathode interface [16–18]. It has been shown that Ca lowers the work function of ITO [16] and AZO [17], which allows for these materials to be used as cathodes in inverted OPVCs. Through lowering the cathode work function, electron collection is improved and holes are blocked from reaching the cathode, thereby reducing the leakage current. The optimum Ca thickness is 3 nm, which corresponds to continuous or nearly continuous layers. For thinner layers, Ca exists as isolated islands and leakage currents can take place between them, which may explain the smaller V_{oc} values (Fig. 5). For thicker films, J_{sc} decreases, which is similar to results that were already obtained in the case of inverted solar cells [17]. The authors attribute this effect to possible partly oxidized Ca. Another possible contribution is that increasing Ca thickness results in a reduction of J_{sc} due to a decrease in reflectivity of the cathode.

By comparison with the work cited in Ref. [17], our Ca thin films are slightly thicker, which can be explained by the fact that our Ca films are deposited on the top of the organic films, which means that they are quite rough, while in the case of Ref. [17] they are immediately deposited onto the ITO bottom electrode.

The interest in the hybrid CBL is that it allows cumulative advantages for both of its constituents. The Alq_3 EBL blocks the excitons and protects the organic electron acceptor from cathode diffusion during its deposition. In the presence of Ca, an Alq_3 thickness of 6 nm appears sufficient. On the other hand, Ca allows a good band matching with a decrease in the series resistance. Moreover, it is thin enough to prevent reflection loss. Therefore, the thin layer of Alq_3 permits the improvement expected from a classical organic EBL, while the low work function of the ultrathin Ca layer induces high electron-collection efficiency without diminishing the cathode reflectivity.

5 Conclusion A new oligomer derivative, BSTV, synthesized by using the McMurry reaction starting from 5″-dimethyl-2, 2′,3′,2″-terthiophene-5′-carbaldehyde, was used as ED in OPVCs. It is shown that promising results are achieved when optimized devices using buffer layers are thermally deposited. The optimum BSTV thickness is 22 nm. For thicker branched BSTV films, the BSTV resistivity induces a decrease in J_{sc}, while when this film is thinner, V_{oc} and J_{sc} decrease due to possible inhomogeneities which may induce some V_{oc} decrease and a smaller light absorption which induces J_{sc} limitation. The study dedicated to the CBL shows that the optimum bilayer structure corresponds to Alq_3 (6 nm)/Ca (3 nm). The short lifetime of the improvement due to Ca shows that it is necessary to look for encapsulating barrier layers with very low oxygen and water permeability.

References

[1] J. C. Bernède, J. Chilean Chem. Soc. **53**, 1549 (2008).
[2] P. Kumar and S. Chand, Prog. Photovolt.: Res. Appl. **20**, 377 (2012).
[3] F. C. Krebs, Sol. Energy Mater. Sol. Cells **93**, 394 (2009).
[4] R. Fitzner, C. Elschner, M. Weil, C. Uhrich, C. Körner, M. Riede, K. Leo, M. Pfeiffer, E. Reinold, E. Mena-Osteritz, and P. Bäuerle, Adv. Mater. **24**, 675 (2012).
[5] Y. Abe, T. Yokoyama, and Y. Matsuo, Org. Electron. **14**, 3306 (2013).
[6] A. Godoy, L. Cattin, L. Toumi, F. R. Diaz, M. A. del Valle, G. M. Soto, B. Kouskoussa, M. Morsli, K. Benchouk, A. Khelil, and J. C. Bernède, Sol. Energy Mater Sol. Cells **94**, 648 (2010).
[7] J. Ouerfelli, S. OuroDjobo, J. C. Bernède, L. Cattin, M. Morsli, and Y. Berredjem, Mater. Chem. Phys. **112**, 198 (2008).
[8] L. Cattin, F. Dahou, Y. Lare, M. Morsli, R. Tricot, S. Houari, A. Mokrani, K. Jondo, A. Khelil, K. Napo, and J. C. Bernède, J. Appl. Phys. **105**, 034507 (2009).
[9] J. C. Bernède, L. Cattin, and S. Morsli, Technol. Lett. **1**, 5 (2014).
[10] J. C. Bernède, L. Cattin, M. Makha, V. Jeux, P. Leriche, J. Roncali, V. Froger, M. Morsli, and M. Addou, Sol. Energy Mater. Sol. Cells **110**, 107 (2013).
[11] M. Makha, L. Cattin, S. Dabos-Seignon, E. Arca, J. Velez, N. Stephan, M. Morsli, M. Addou, and J. C. Bernède, Indian J. Pure Appl. Phys. **51**, 569 (2013).
[12] A. Mishra and P. Bäuerle, Angew. Chem. Int. Ed. **51**, 2020 (2012).
[13] B. P. Rand, J. Li, J. Xue, R. J. Holmes, M. E. Thompson, and S. R. Forrest, Adv. Mater. **17**, 2714 (2005).
[14] J. Wagner, M. Gruber, A. Wilke, Y. Tanaka, K. Topczak, A. Steindamm, U. Hörmann, A. Opitz, Y. Nakayama, H. Ishii, J.

Pflaum, N. Koch, and W. Brütting, J. Appl. Phys. **111**, 054509 (2012).
[15] Y. Liu, Q. Ren, Z. Su, B. Chu, W. Li, S. Wu, F. Jin, B. Zhao, X. Yan, J. Wang, D. Fan, and F. Zhang, Org. Electron. **13**, 2156 (2012).
[16] D. W. Zhao, S. T. Tan, L. Ke, P. Liu, A. K. K. Kyaw, X. W. Sun, G. Q. Lo, and D. L. Kwong, Sol. Energy Mater. Sol. Cells **94**, 985 (2010).
[17] D. Chen, C. Zhang, Z. Wang, J. Zhang, S. Tang, W. Wei, L. Sun, and Y. Hao, Org. Electron. **15**, 3006 (2014).
[18] Z. Wang, C. Zhang, D. Chen, D. Chen, S. Tang, J. Zhang, L. Sun, T. Heng, and Y. Hao, Int. J. Photoenergy ID 209206 (2014).
[19] F. Martinez, G. Neculqueo, J. C. Bernéde, L. Cattin, and M. Makha, Technol. Lett. **1**, 5 (2014).
[20] M. Jenart, C. Niebel, J.-Y. Balandier, J. Leroy, A. Mignolet, S. Stas, A. Van Vooren, J. Cornil, and Y. H. Geerts, Tetrahedron **68**, 349 (2012).
[21] Y. Berredjem, N. Karst, L. Cattin, A. Lkhdar-Toumi, A. Godoy, G. Soto, F. Diaz, M. A. Del Valle, M. Morsli, A. Drici, A. Boulmokh, A. H. Gheid, A. H. Gheid, A. Khelil, and J. C. Bernède, Dyes Pigments **78**, 148 (2008).
[22] Y. Lare, B. Kouskoussa, K. Benchouk, S. OuroDjobo, L. Cattin, F. R. Diaz, M. Gacitua, T. Abachi, M. A del Valle, F. Amijo, G. A. East, and J. C. Bernède, J. Phys. Chem. Solids **72**, 97 (2011).
[23] Q. L. Song, F. Y. Li, H. Yang, H. R. Wu, X. Z. Wang, W. Zhou, J. M. Zhao, X. M. Ding, C. H. Huang, and X. Y. Hou, Chem. Phys. Lett. **416**, 42 (2005).
[24] R. F. Salzman, J. Xue, B. P. Rand, A. Alexander, M. E. Thompson, and S. R. Forrest, Org. Electron. **6**, 242 (2005).
[25] L. Cattin, J. C. Bernède, Y. Lare, S. Dabos-Seignon, N. Stephant, M. Morsli, P. P. Zamora, F. R. Diaz, and M. A. del Valle, Phys. Status Solidi A **210**, 802 (2013).
[26] G. Dennler, C. Lungenschmied, H. Neugebauer, N. S. Sariciftci, M. Latrèche, G. Czeremuszkin, and M. R. Wertheimer, Thin Solid Films **511–512**, 349 (2006).
[27] A. Latef and J. C. Bernède, Phys. Status Solidi A **124**, 243 (1991).
[28] Y. Berredjem, N. Karst, A. Boulmokh, A. H. Gheid, A. Drici, and J. C. Bernède, Eur. Phys. J. **40**, 163 (2007).
[29] M. O. Reese, S. A. Gevorgyan, M. Jørgensen, E. Bundgaard, S. R. Kurtz, D. S. Ginley, D. C. Olson, M. T. Lloyd, P. Morvillo, E. A. Katz, A. Elschner, O. Haillant, T. R. Currier, V. Shrotriya, M. Hermenau, M. Riede, K. R. Kirov, G. Trimmel, T. Rath, O. Inganäs, F. Zhang, M. Andersson, K. Tvingstedt, M. Lira-Cantu, D. Laird, C. McGuiness, S. J. Gowrisanker, M. Pannone, M. Xiao, J. Hauch, R. Steim, D. M. DeLongchamp, R. Rosch, H. Hoppe, N. Espinosa, A. Urbina, G. Yaman-Uzunoglu, J.-B. Bonekamp, A. J. J. M. van Breemen, C. Girotto, E. Voroshazi, and F. C. Krebs, Sol. Energy Mater. Sol. Cells **95**, 1253 (2011).
[30] J. Kim and S. Yim, Appl. Phys. Lett. **99**, 193303 (2011).
[31] H.-W. Lin, H.-W. Kang, Z.-Y. Huang, C.-W. Chen, Y.-H. Chen, L.-Y. Lin, F. Lin, and K.-T. Wong, Org. Electron. **13**, 1925 (2012).
[32] P. P. Zamora, F. R. Díaz, M. A. del Valle, L. Cattin, G. Louarn, and J. C. Bernède, Nat. Resources **4**, 123 (2013).
[33] M. Makha, L. Cattin, S. Dabos-Seignon, E. Arca, J. Velez, N. Stephan, M. Morsli, M. Addou, and J. C. Bernède, Indian J. Pure Appl. Phys. **51**, 568 (2013).